E949 Technical Note K-xxx

The Active Degrader

Ilektra A. Christidi, Stony Brook

June 9, 2006

Abstract

The Active Degrader (AD) has not been used in the PNN1 analysis, but is essential for PNN2, given the expected photon distribution from target-scattered Kp2 events, which is uniform in dip angle. Sure enough, photon activity is evident for Kp2 and kink events.

1 Formalities

In the following, "energies" are in arbitrary units. For the CCDs they are the pulse height (average of the 2 highest bins of the pulse found by the pulse.f routine) and they have been calibrated with respect to each other and pedestal-corrected for multiple hits in one CCD. The ADCs are also calibrated with respect to each other and then de-multiplexed based on the CCD information. A value is assigned in every sector (not every hit), corrected also for the energy lost in dead material when multiple sectors are crossed.

Beam particle track extrapolation is done to find which AD sectors are expected to be transversed by the incoming K, and thus have some energy deposit associated with the beam. In principle, these sectors should be excluded for PV purposes (more on that later). The incoming xy point is found by extrapolating the line defined by the hit points in BWC1 and BWC2 to the US face of the AD. The outgoing point is the one given by the B4 hit coordinates. Every sector between these 2 points is assigned to the K path.

When slewing corrections were applied to the TDCs and CCDs, the time resolutions were not improved significantly but the distributions were distorted, therefore it was decided not to use the corrections. The relative timing between different sectors fluctuated by about 200ps at most, so this was not deemed to be a neccessary correction either.

The acceptance sample used in these studies is Km21 monitors, with KINCUTS, PSCUT02 and KMU2BOX cut applied, where no photon or beam activity is expected. Two rejection samples were used: Kp2 peak events from SKIM5 (without TDCUT), with KINCUTS, PSCUT02, KPI2BOX, loose PVCUT and TGCUTS, and "good" (kink point in the target) kinks from SKIM8 with SKIM5 cuts (without TDCUT), KINCUTS, PSCUT02_KINK, $ptot < 225 MeV/c$, loose PVCUT, loose TGCUTS and DELCO3.

2 Timing peaks in the AD

In fig.1-4, the time distributions of hits in the AD are shown in black for the acceptance sample and red for the rejection samples (Kp2 peak on the left and kinks on the right). All the histograms are normalized to the number of events/incoming Kaons. As can be seen in fig. 1, which is for sectors on the K path, the behaviour of the 3 samples is effectively the same in terms of K activity. The upper plots are the times with respect to tk, where an on-time peak with 1.3ns sigma is obvious, and the lower ones with respect to tpi, which show a decay lifetime shape. fig. 2 shows the same distributions for sectors off the K path. In addition to some K activity remnants in time with tk, that are the same for all samples (probably due to flaws in the path extrapolation algorithm), a strong photon peak with 2ns sigma is present about 2ns after tpi for the rejection samples only. fig. 3 and fig. 4 show the same for the CCDs, which have a similar resolution (1.7ns for the K peak and 2.6ns for the photon one) and a smaller shift (1.3ns) with respect to tpi. This is probably because the CCD time is the one at the 40% rising point of the pulse, returned by pulse.f.

The 2ns shift of the photon timing peak from tpi has been extensively investigated. Fig. 5 shows the dependence of the fitted peak position on tgz (and thus the distance the photons have to travel from the target until they reach the AD), which has a clear linear form. For the TDCs, the slope of the linear fit gives a pretty good speed of light value of about $3.3 \times 10^8 m/s$, and for the CCDs a worse one. From these results, the photon TOF accounts for about 1ns.

During the time slewing studies, it was noted that, although the energy spectra of the K's and the photons (to be shown later) differ significantly, this effect does not account for the shift of the two timing peaks, as they are consistently different by 2ns at any restricted energy range.
The difference of tpi from the time of individual pi fibers does not show a systematic shift either, but it is dominated by the resolution (if the fibers closest to the vertex were consistently earlier than tpi, this would reveal a consistent difference between the real time that the photon was emitted and left a trace in the AD, and the average pion time, namely tpi). So, the remaining 1ns shift remains a mystery.

3 Applying the cut

Based on the time and energy distributions in the AD, different ways to apply a PV cut were investigated. The main idea is to add the energy deposited either in whole sectors (for ADCs) or individual hits (for CCDs) and veto events based on this sum. For the ADCs, the different schemes are using sectors with hits (a) in time with tpi (-2ns to 8ns) (b) in time with tpi and no other hits (c) in time with tpi and out of the K path and (d) in time with tpi, no other hits and out of the K path. For the CCDs, either hits (a) in time with tpi or (b) in time with tpi and in sectors out of the K path were used. The results, in the form of acceptance*rejection vs energy threshold, are shown in fig. 6 for the Kp2 peak and in fig. 7 for the kinks. For both the rejection samples, cutting on the sum of CCD "energy" at 5., irrespective of the sector the hit belongs to, seems to be the favorable case.

These rej*acc graphs also shed light on the question of how much photon activity is hidden under the Kaon sectors and how efficiently we can veto on it (losing the least acceptance) by using CCD pulse fits. It is evident that even if we veto on *any* activity at tpi in K sectors, the acceptance loss is offseted by the rejection gain. More detail is available in fig. 8 and fig. 9, which show the multiplicity (number of sectors hit) of the K, based on its extrapolated track and its timing, as well as the photon at TRS for KP2 peak events. 2 sectors on average are hit by the K and 2 by the gamma (with non-zero energy deposit). The number of sectors on the K path that have also non-zero energy hits at TRS is also shown, by itself and as a function of the total number of sectors with non-zero hits at TRS. Finally, the energy deposited in all sectors at TRS vs the energy only in the ones transversed by the Kaon is plotted. It turns out, from the number of events in the diagonal of the 2 last plots, which are the ones that all the photon activity is hidden under the Kaon, that, from the events that have photon energy hidden under the K sectors, only about 10% do not have significant energy outside these sectors to veto on.

4 Radius dependence of the energy

The dependence of the energy measured by the AD on the distance of the incoming track from the center of the detector was investigated. This is expected to vary by up to a factor of 2-3, as is shown in fig. 10, where the mean of the ADC energy distribution of incoming Kaons is ploted vs the distance of the trace of the incoming particle left in the B4 from the center, for Km2 events where the track is confined in one sector. The same trend is present for the CCDs (fig. 11), although the shape variation of the pulse with the distance from the readout may be to blame for the weakest dependence and the saturation for large distances (remember, the CCD “energy” is the pulse height).

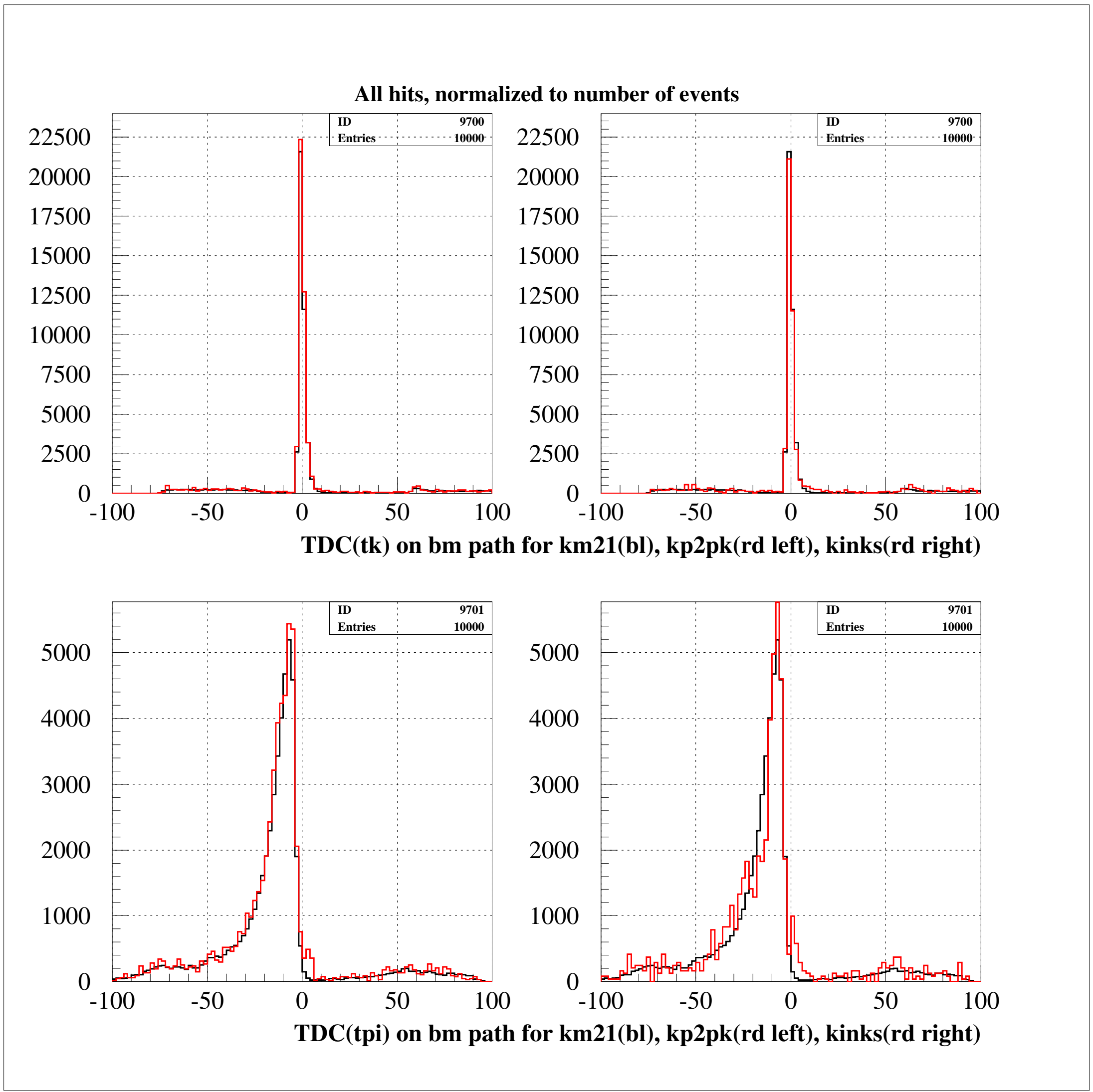

Figure 1: Time distributions of the TDC hits with respect to tk (top row) and tpi (bottom row) for sectors on the incoming Kaon path. Black histograms are for the acceptance sample (Km2 monitors) and red for the 2 rejection samples (Kp2peak on the left and kinks on the right).

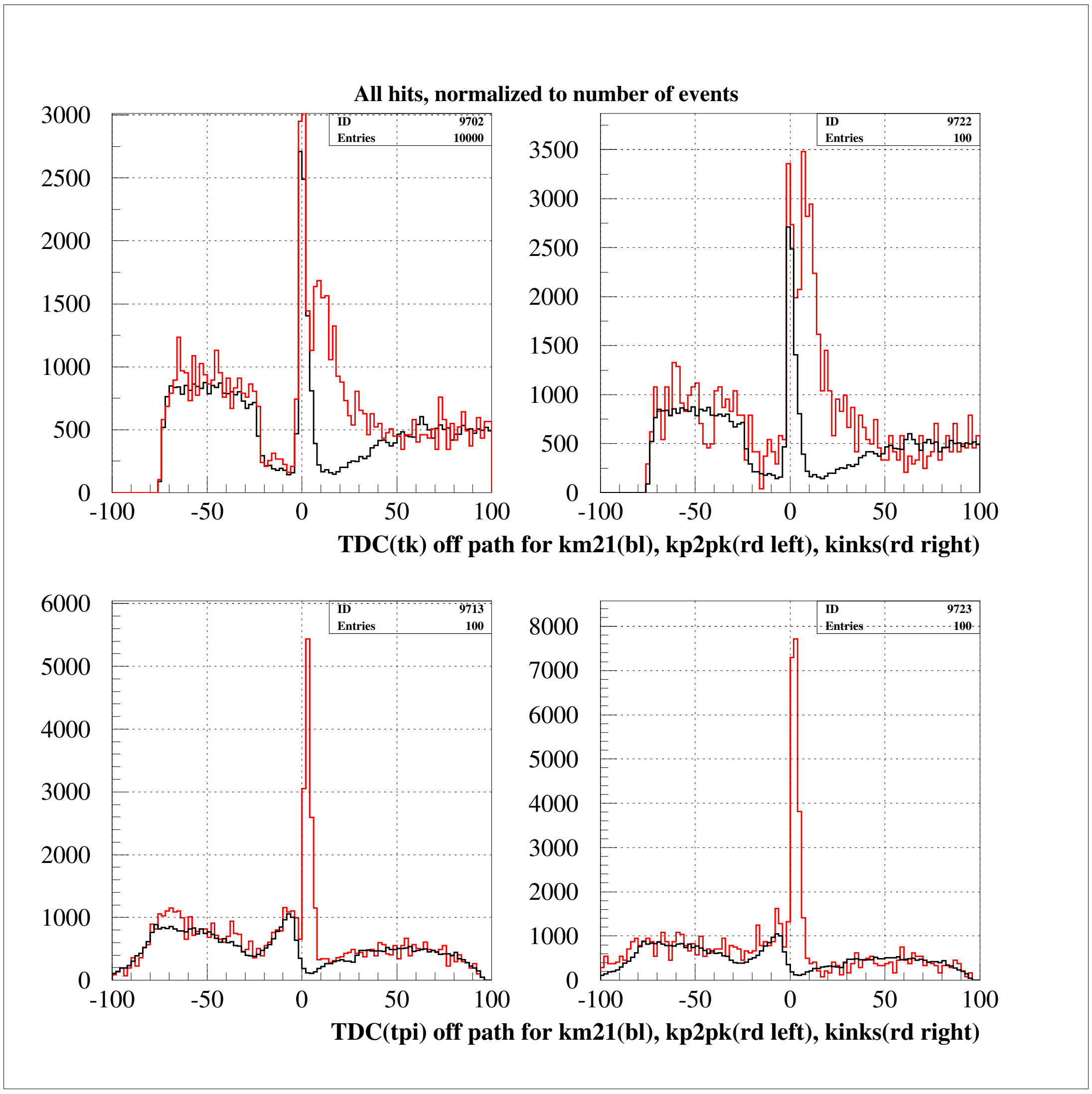

Figure 2: Time distributions of the TDC hits with respect to tk (top row) and tpi (bottom row) for sectors off the incoming Kaon path. Black histograms are for the acceptance sample (Km2 monitors) and red for the 2 rejection samples (Kp2peak on the left and kinks on the right).

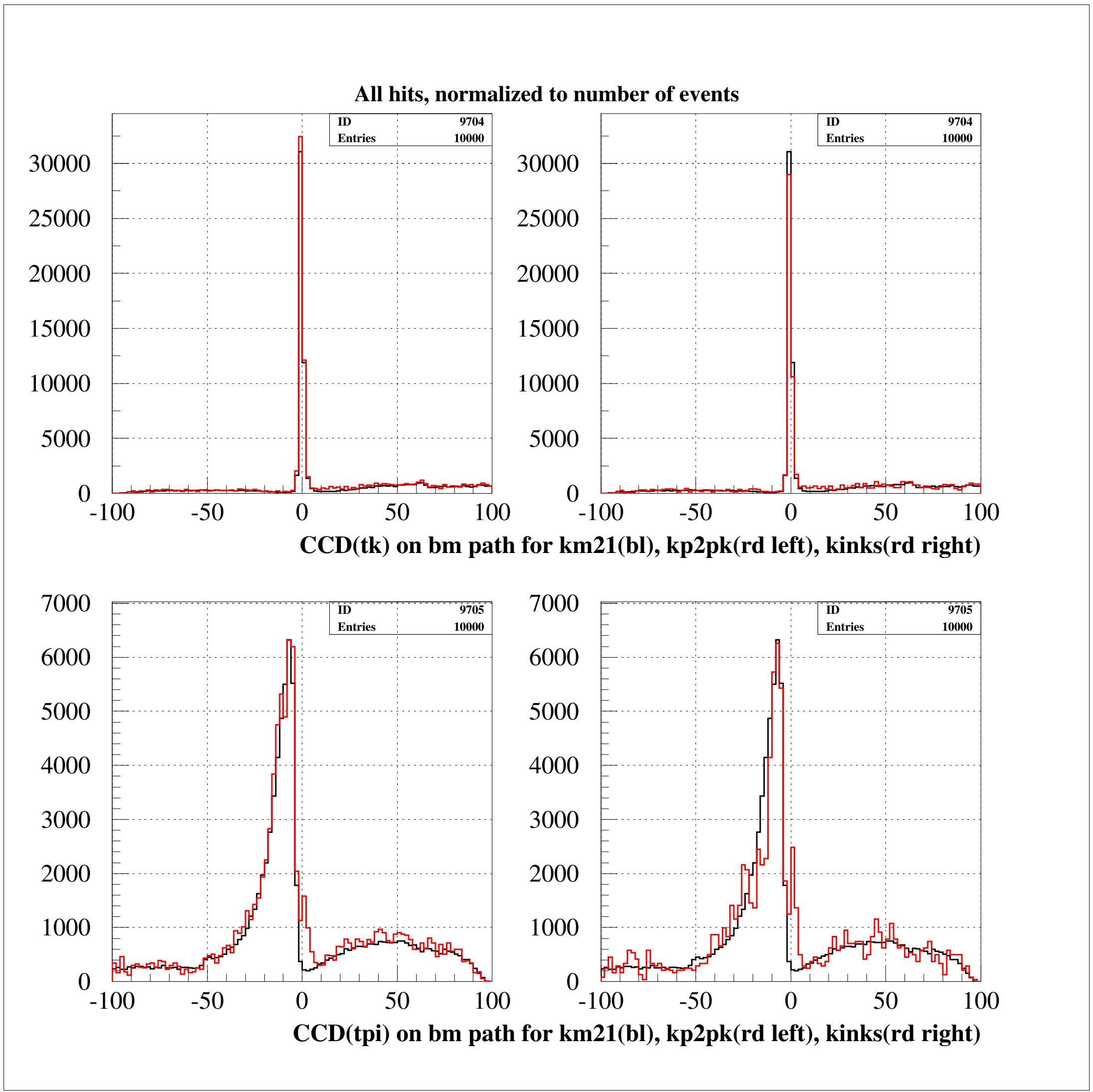

Figure 3: Time distributions of the CCD hits with respect to tk (top row) and tpi (bottom row) for sectors on the incoming Kaon path. Black histograms are for the acceptance sample (Km2 monitors) and red for the 2 rejection samples (Kp2peak on the left and kinks on the right).

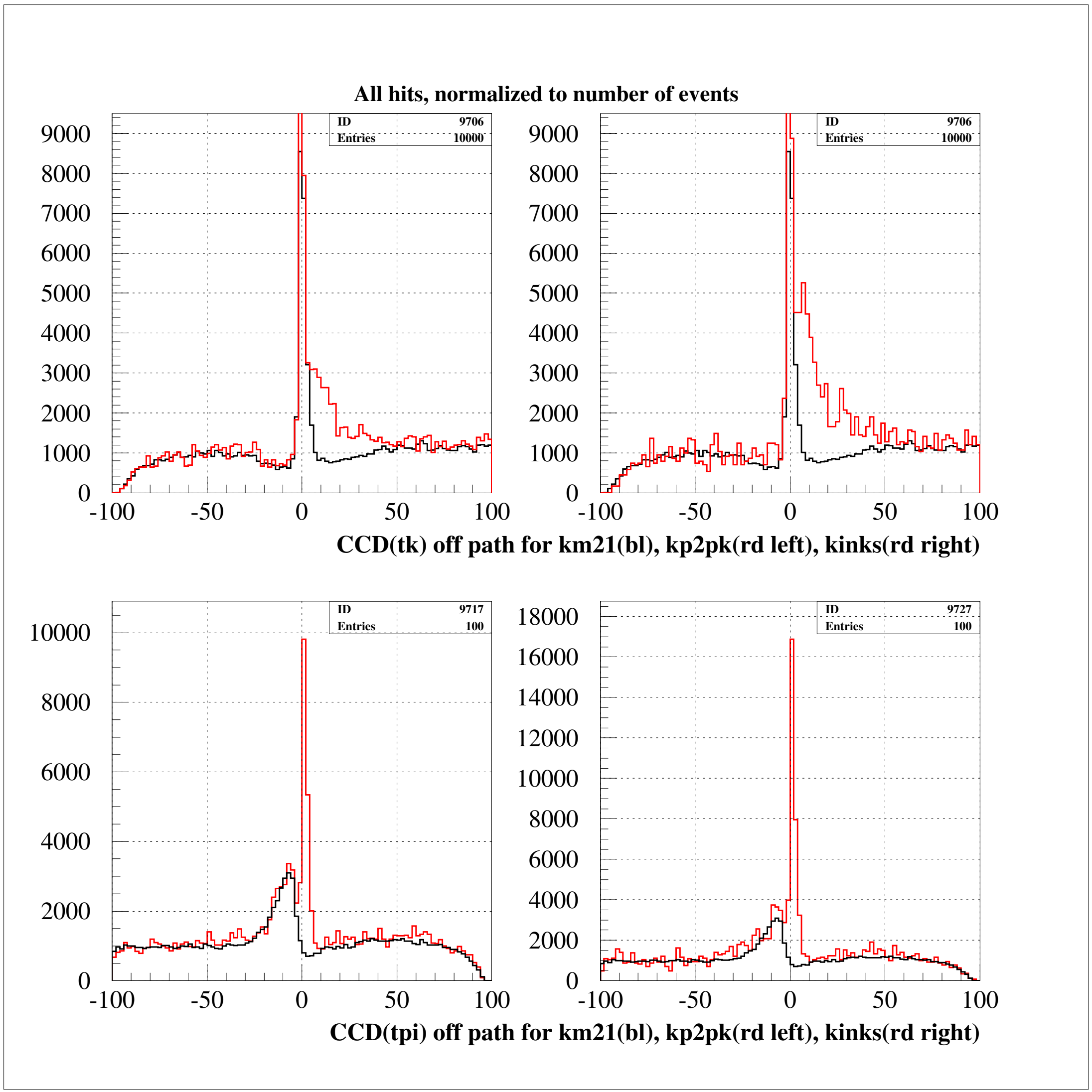

Figure 4: Time distributions of the CCD hits with respect to tk (top row) and tpi (bottom row) for sectors off the incoming Kaon path. Black histograms are for the acceptance sample (Km2 monitors) and red for the 2 rejection samples (Kp2peak on the left and kinks on the right).

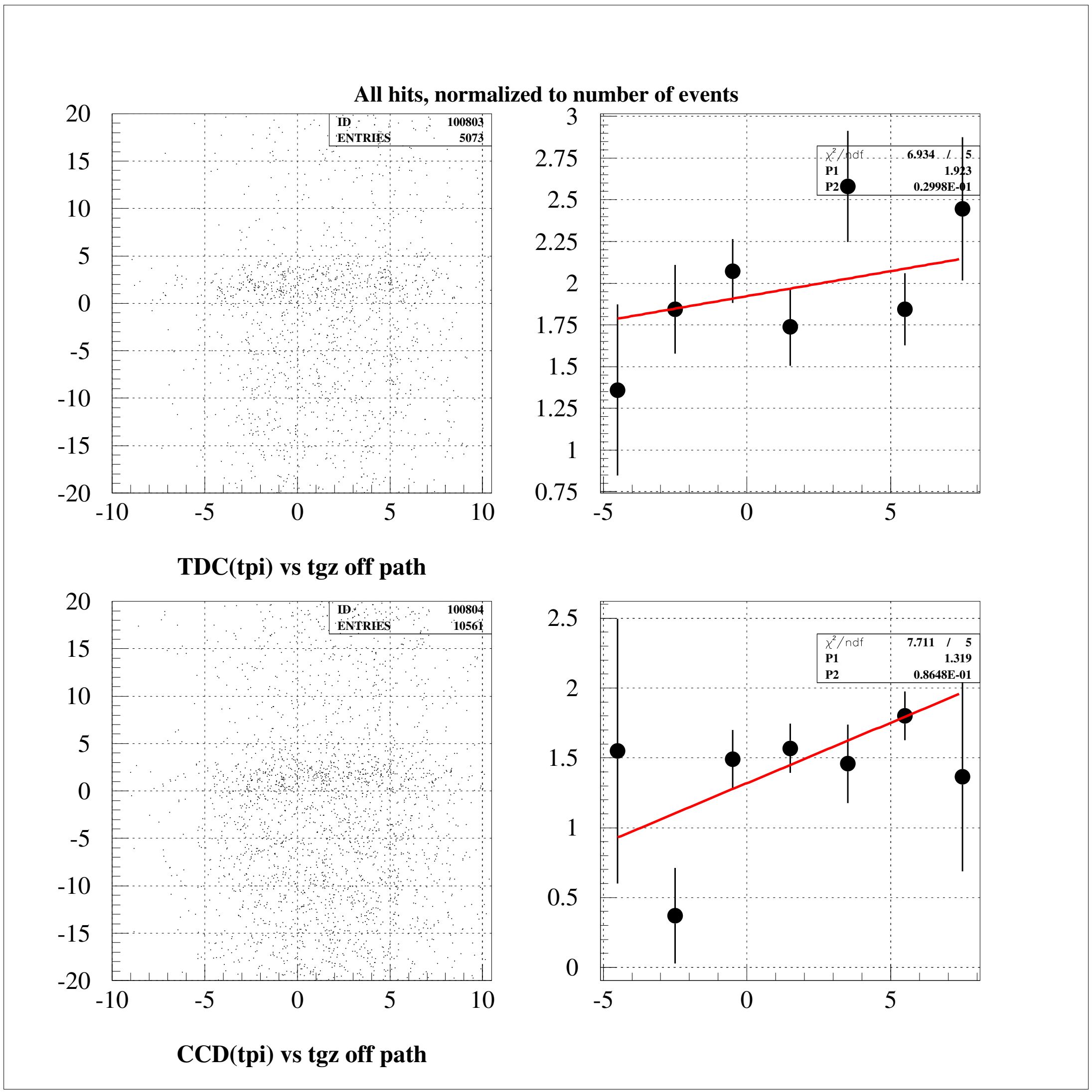

Figure 5: Dependence of the photon peak position in time with repsect to tpi, on tgz. Scatter plots and fitted (within -2.ns and 6.ns) mean times vs tgz are shown for the TDCs in the top and CCDs in the bottom row.

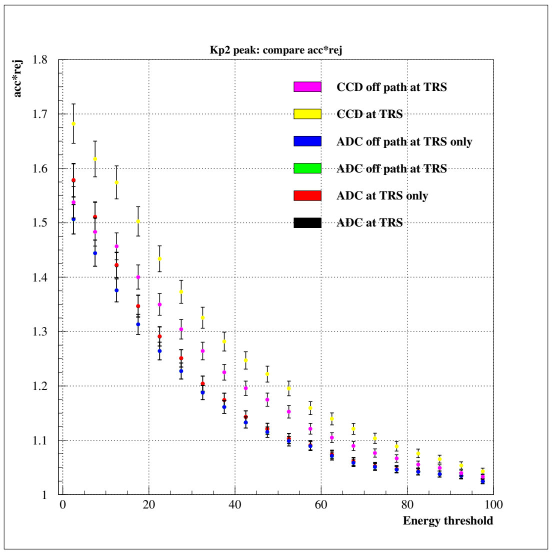

Figure 6: Acceptance*rejection vs total ADC or CCD energy threshold, for different sector selection, for Kp2 peak events.

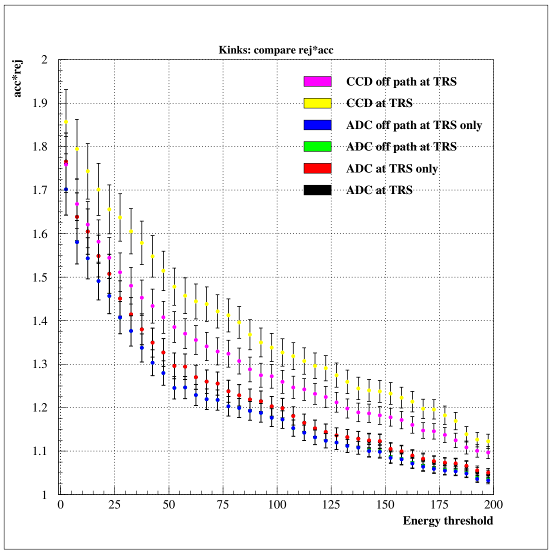

Figure 7: Acceptance*rejection vs total ADC or CCD energy threshold, for different sector selection, for kink events.

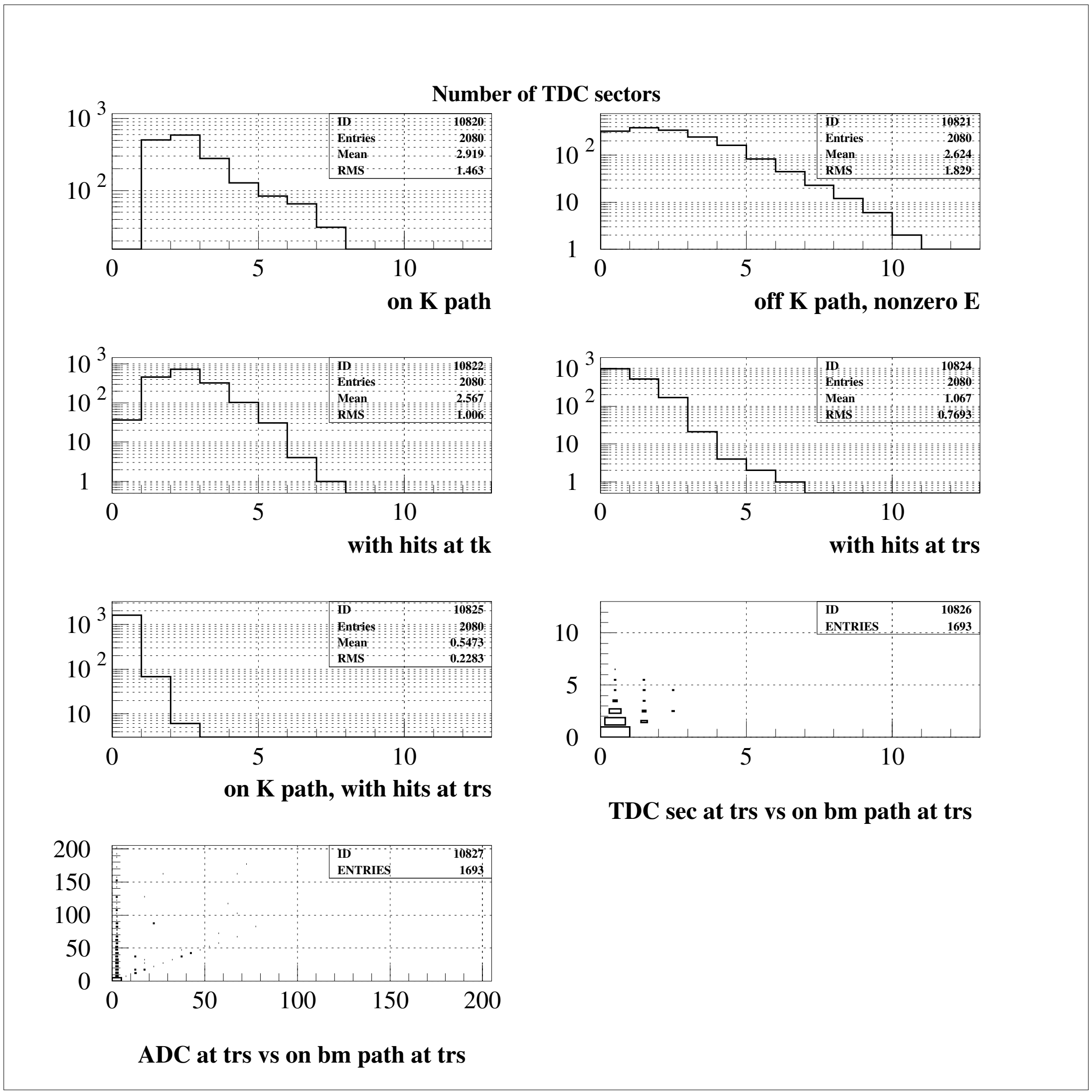

Figure 8: Number of sectors hit by incoming Kaons and outgoing photons: (a) on the extrapolated K path (b) off the extrapolated K path with non-zero ADC energy deposit (c) with TDC hits in time with tk (d) with TDC hits in time with TRS (e) with TDC hits in time with TRS on the extrapolated K path (f) number of sectors with TDC hits in time with TRS vs number of sectors with TDC hits in time with TRS on the extrapolated K path (g) total ADC energy deposited at sectors with hits at TRS vs total ADC energy deposited at sectors with hits at TRS on the K path.

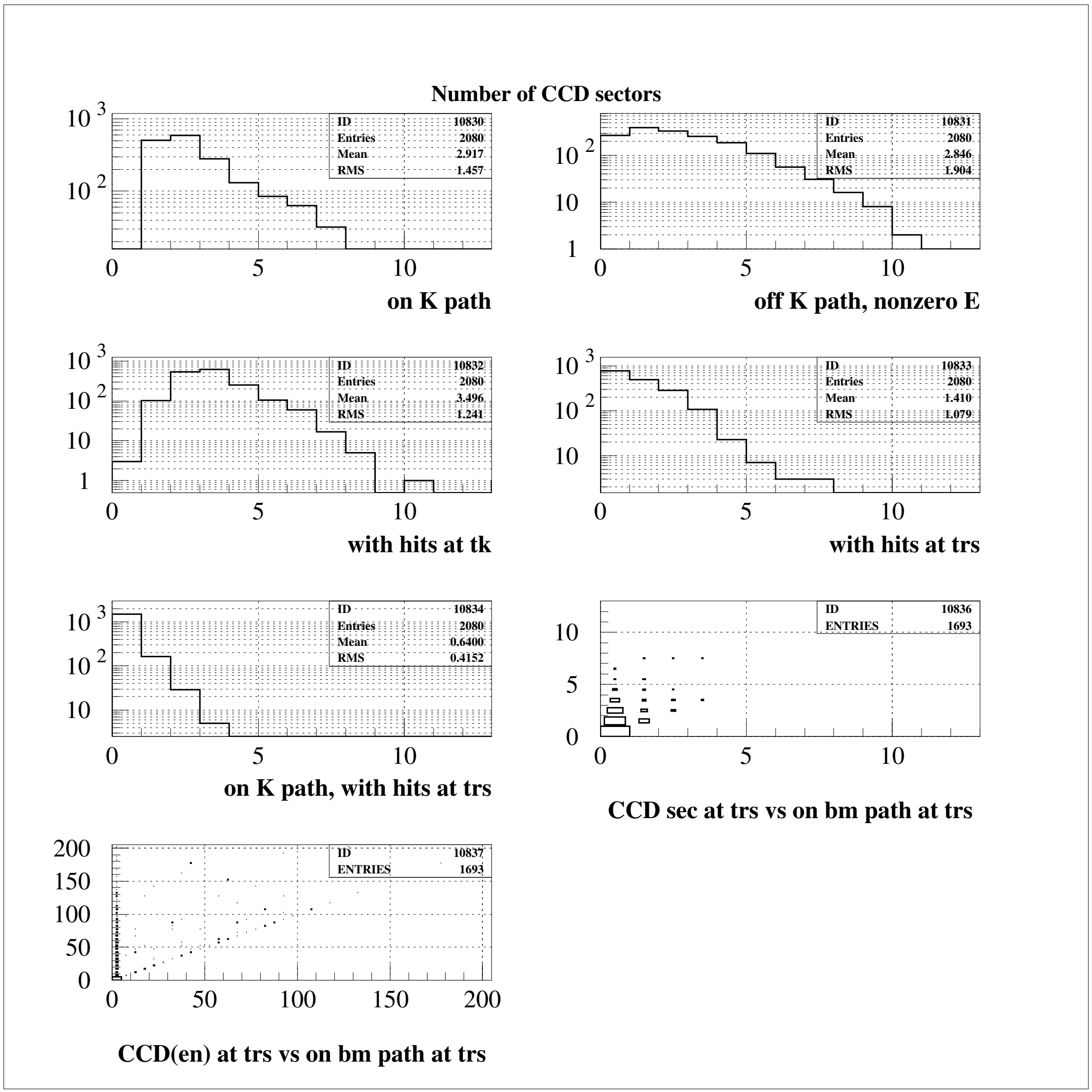

Figure 9: Number of sectors hit by incoming Kaons and outgoing photons: (a) on the extrapolated K path (b) off the extrapolated K path with non-zero CCD energy deposit (c) with CCD hits in time with tk (d) with CCD hits in time with TRS (e) with CCD hits in time with TRS on the extrapolated K path (f) number of sectors with CCD hits in time with TRS vs number of sectors with CCD hits in time with TRS on the extrapolated K path (g) total CCD energy deposited at sectors with hits at TRS vs total CCD energy deposited at sectors with hits at TRS on the K path.

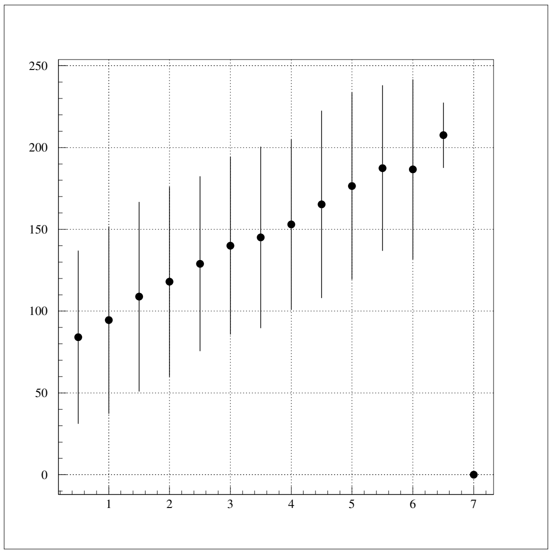

Figure 10: Mean of the ADC energy distribution of incoming K's vs the distance of the trace of the incoming particle left in the B4 from the center.

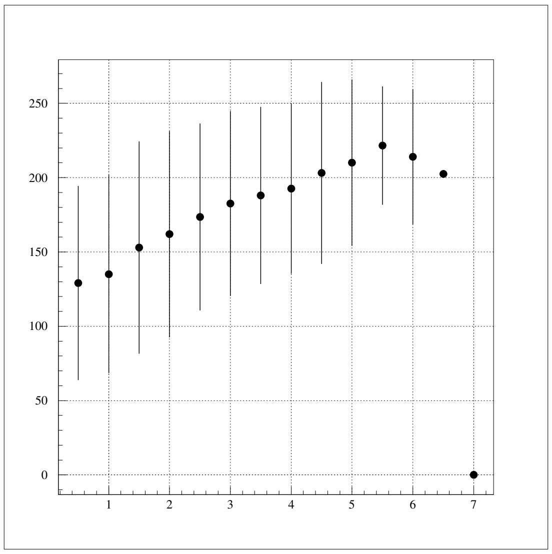

Figure 11: Mean of the CCD energy distribution of incoming K's vs the distance of the trace of the incoming particle left in the B4 from the center.